THE GEOLOGICAL SOCIETY OF AMERICA®

Exceptional preservation of organic matrix and shell microstructure in a Late Cretaceous *Pinna* fossil revealed by photoemission electron spectromicroscopy

Corinne E. Myers[1]*, Kristin D. Bergmann[2], Chang-Yu Sun[3], Nicholas Boekelheide[2], Andrew H. Knoll[4], and Pupa U.P.A Gilbert[3,5]*

[1]University of New Mexico, Department of Earth and Planetary Sciences, Albuquerque, New Mexico 87131, USA
[2]Massachusetts Institute of Technology, Department of Earth, Atmospheric and Planetary Sciences, Cambridge, Massachusetts 02139, USA
[3]University of Wisconsin–Madison, Department of Physics, Madison, Wisconsin 53706, USA
[4]Harvard University, Department of Organismic and Evolutionary Biology, Cambridge Massachusetts 02138, USA
[5]University of Wisconsin–Madison, Departments of Chemistry and Geoscience, Madison, Wisconsin 53706, USA

ABSTRACT

We present evidence of exceptional preservation in the nacre and prismatic layers of a 66 Ma bivalve shell using photoemission electron spectromicroscopy (PEEM). PEEM is a novel method to assess *in situ* the quality of mineralogical and organic preservation. The analysis is non-invasive and non-destructive, providing spatially explicit maps of microstructure, organics and mineral components, and the crystallographic orientation in mollusk shells. Comparison of a Late Cretaceous and a modern shell demonstrates that the 66 Ma shell (1) preserves original aragonite and calcite crystals in nacre and prismatic layers, respectively, (2) maintains nearly identical mineral microstructure and crystal orientations, and (3) preserves interprismatic proteins. Remarkably, interprismatic proteins are preserved with intact peptide bonds, and suggest an abundance of the amino acid glycine. These findings in a 66 Ma shell support the exceptional quality of organic preservation documented here, which may prove to be relatively common among fossil shells that preserve nacre. PEEM analysis is useful for understanding taphonomic processes influencing shell and molecular fossil preservation over geologic time scales, and contributes to our knowledge of molluscan physiology, biomineralization, evolution, and diagenesis.

INTRODUCTION

The quality of fossil preservation is a central question in paleobiology, underpinning hypotheses, analyses, and interpretations of data, whether morphological, biogeographic, geochemical, ecological, or evolutionary. Here we examine the preservation of a 66 Ma marine mollusk shell through analysis of its shell microstructure and interprismatic organic constituents, and compare these to a modern shell. Polypeptide chains in fossil organic matrices were first reported in brachiopods by Jope (1969) and in mollusks by Grégoire and Voss-Foucart (1970). In most previous studies, the fossil was demineralized to extract the organic matrix for analysis, thus information regarding the shell microstructure and the location of protein residues was lost; these analyses are also susceptible to lab contamination. More recently, peptide bonds and chitin-protein complexes have been observed in Jurassic dinosaur bone collagen and Paleozoic arthropod cuticle, respectively (Cody et al., 2011; Lee et al., 2017; Schroeter et al., 2017). Amino acid and protein residues have also been documented in Pleistocene horse bone (Orlando et al., 2013). *In situ* protein chains have not been definitively described in the biominerals of pre-Cenozoic marine mollusks—perhaps the most abundant animal fossils (although, see Zhao et al. [2003] for a disputed example). Indirect evidence of proteins in Cretaceous mollusks (e.g., De Jong et al., 1974; Weiner et al., 1976) has been inferred from chromatography and immunoreactivity experiments (however, see Muyzer and Westbroek [1989] for a spatial analysis of Pleistocene biopolymers in bivalves using immunohistochemical staining).

Most previous work focused on specimens from fossil *Lagerstätten*, deposits with exceptional preservation that may include soft parts (e.g., Grégoire and Voss-Foucart, 1970; Weiner et al., 1976; Cody et al., 2011). In contrast, we observe preservation of interprismatic organics in a mollusk shell that preserves nacre (termed here the "nacre-grade" taphonomic window) from an otherwise unexceptional geological setting. Although less resilient than shells composed solely of calcite, nacreous shells extend back to the Paleozoic (Vendrasco et al., 2013) and are not uncommon in the Mesozoic (Gilbert et al., 2017). Nacre preservation does not represent an extreme or rare quality of preservation; therefore, the organic compounds observed in the interprismatic matrix (IM) may prove to be relatively common among fossil mollusk shells with nacre. A better understanding of the quality of nacre-grade preservation may aid research in geochemistry, paleobiology, and taphonomy by, for example, improving confidence in stable isotope values of nacreous materials, inferences on the evolution of shell morphology or biomineralization, and comparisons between taxa in the same taphonomic window (e.g., Weiner et al., 1976; Schweitzer, 2004; Gilbert et al., 2017).

METHODS

Two specimens of bivalve shell were analyzed here: one *Pinna nobilis* (Harvard Museum of Comparative Zoology sample MCZ-371544) collected live in 1991, and one *Pinna* sp. (American Museum of Natural History sample AMNH-99982) from the Late Cretaceous Owl Creek Formation, Mississippi, USA (ca. 66 Ma). Both specimens were prepared for analysis following standardized methods, and analyzed as described by Gilbert et al. (2017), using photoemission electron spectromicroscopy (PEEM). PEEM enables acquisition of X-ray absorption near-edge structure (XANES) spectroscopy (Stöhr, 2013) and polarization-dependent imaging contrast (PIC) mapping (Gilbert et al., 2011); it is possible to observe characteristics of shell microstructure, mineralogy, and organic compounds within the same experiment. XANES spectroscopy via PEEM nondestructively identifies minerals and organics *in situ* using spatially explicit high-resolution spectroscopy (Metzler et al., 2010). Thus, the

*E-mail: cemyers@unm.edu; pupa@physics.wisc.edu

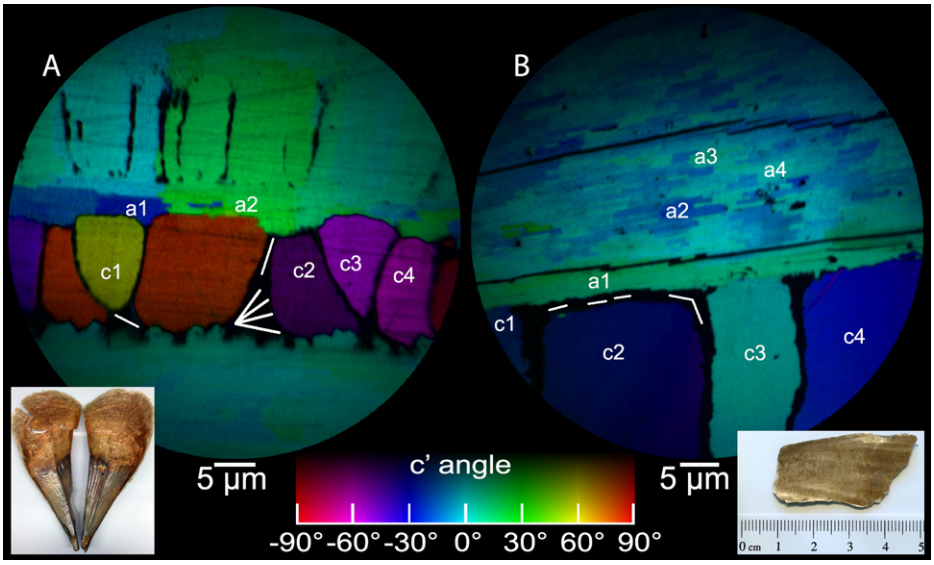

Figure 1. Polarization-dependent imaging contrast (PIC) maps of modern and fossil *Pinna* shells. Colors indicate the in-plane angles, and brightness indicates the off-plane angles formed by the crystallographic c-axis and the polarization plane. The c-axis projected onto the polarization plane is termed the *c′*-axis, and the angle it forms with the vertical in the polarization plane is termed the *c′* angle. See the Data Repository [footnote 1] for more detail on this method. A: Modern *Pinna nobilis*; prismatic calcite at the center, nacre at top and bottom. B: Late Cretaceous *Pinna* sp.; prismatic calcite at bottom, nacre on top. Specimen insets are shown with greater detail in Fig. DR1 (see footnote 1). Figure 2 spectra were extracted from regions "a" (aragonite),"c" (calcite), and along the white lines.

likelihood of lab contamination is minimized (Lee et al., 2017). Analyses were run on beamline 11.0.1.1 and the PEEM-3 microscope at the Advanced Light Source, Lawrence Berkeley National Laboratory (California, USA). PEEM was used in two modes: (1) as a spectromicroscope to identify organics or minerals (carbon K-edge and oxygen K-edge XANES, respectively), and (2) as a PIC mapper to measure crystal orientations. Analytical methods are described in detail in the GSA Data Repository[1], and by Gilbert et al. (2017).

RESULTS

Figure 1 shows PIC maps of modern and Late Cretaceous *Pinna* shells, highlighting nacre tablets and calcite prisms. Whereas calcite prisms have randomly oriented crystals, aragonite crystals in nacre can be initially mis-oriented near the nacre-prismatic boundary, but gradually become co-oriented within ±15° (Gilbert et al., 2008; Olson et al., 2013). This is visible at the top of both panels in Figure 1 (tablet colors vary only between greenish- and bluish-cyan). Comparison of the modern and fossil specimen demonstrates nearly identical shell microstructure, including morphology and orientation of all crystals. This finding highlights the excellent quality of preservation in the fossil shell.

Figures 2A and 2B show oxygen K-edge XANES spectra extracted from the regions labeled in Figure 1. These spectra demonstrate that prisms and nacre tablets are indeed calcite and aragonite, respectively. The peaks between 535 eV and 545 eV vary diagnostically between calcite and aragonite. These peaks represent the transition between core shell electrons (1s) to the anti-bonding (*) sigma (σ) molecular orbital. The core electrons are in the oxygen (O) when this is double-bonded to carbon (C, thus C=O). The transition is abbreviated O 1s → $\sigma^*_{C=O}$. We observe the characteristic 3 σ* peaks in calcite and 5 σ* peaks in aragonite (arrows in Figs. 2A and 2B). The σ* peak intensities are always anti-correlated with those of π* peaks (anti-bonding [*] pi orbital [π], abbreviated π*), and depend on crystal orientation for both calcite and aragonite (Gilbert et al., 2017).

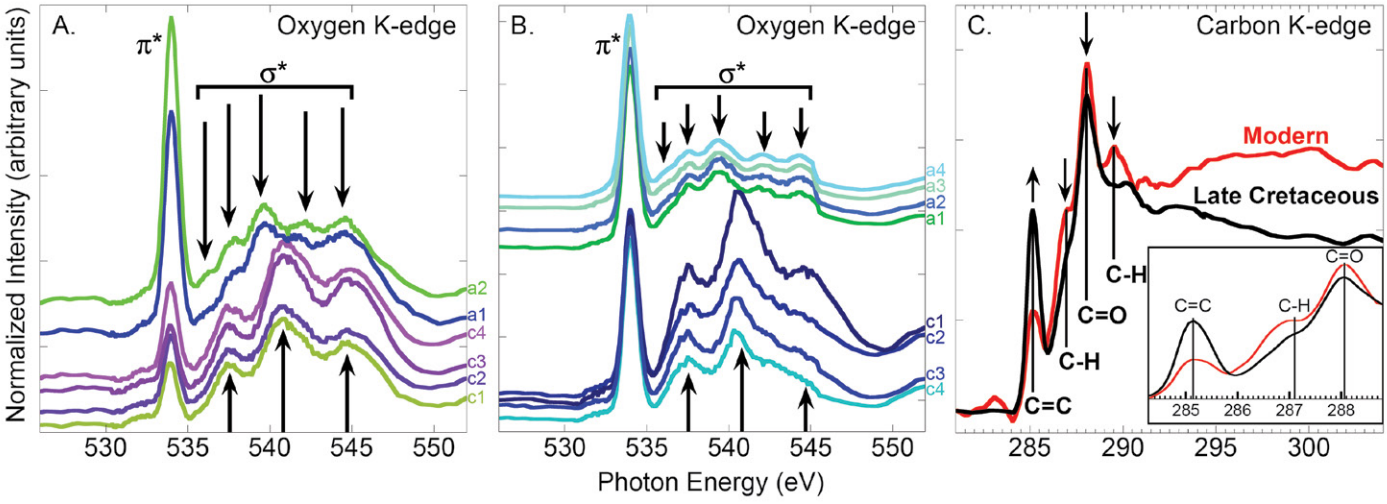

Figure 2. Oxygen and carbon K-edge X-ray absorption near-edge structure (XANES) spectra. Oxygen spectra were extracted from the "a" and "c" regions in Figure 1 for the modern (A) and fossil (B) shell; carbon spectra (C) were extracted from the white lines in Figure 1. In A and B, downward arrows indicate the 5 σ* (anti-bonding [*] σ molecular orbital) peaks diagnostic of aragonite, and upward arrows indicate the 3 σ* peaks diagnostic of calcite. In C, the π* (anti-bonding π orbital) peak positions are 285.1 eV (C=C), 287.1 eV (C-H), 288.1 eV (C=O) (magnified in the inset); the σ* peak is at 289.5 eV (C-H) (C—carbon; H—hydrogen; O—oxygen). Arrows indicate peaks that increase or decrease when comparing the fossil to the modern shell.

[1]GSA Data Repository item 2018258, detailed description of analytical methods, and Figure DR1 (detailed images of specimens, including location and size of analyzed samples), is available online at http://www.geosociety.org/datarepository/2018/, or on request from editing@geosociety.org.

The unexpected observation of such excellent microstructure preservation (Fig. 1) prompted us to analyze the organics also using PEEM. Figure 2C shows carbon K-edge XANES spectra exclusively from organics in Figure 1 (white lines). The comparison of modern and Late Cretaceous spectra reveals that both are characteristic of proteins. This includes the expected π* peaks at 285.1, 287.1, and 288.1 eV (C 1s $\rightarrow \pi^*_{C=C}$, C 1s $\rightarrow \pi^*_{C=H}$, and C 1s $\rightarrow \pi^*_{C=O}$ transitions, respectively), and the σ* peak at 289.5 eV (C 1s $\rightarrow \sigma^*_{C-H}$ transition), which are diagnostic for amino acids (e.g., Boese et al., 1997; Kaznacheyev et al., 2002; Myneni, 2002; Benzerara et al., 2006). The energy of the peak associated with the C=O bond is unusually low, at 288.1 eV. Separate amino acids exhibit this peak at 288.6 eV (Kaznacheyev et al., 2002; Myneni, 2002), whereas amino acid chains in proteins shift this peak to 288.2–288.6 eV (e.g., Boese et al., 1997; Gordon et al., 2003; Brandes et al., 2004). A shift to 288.0–288.2 eV has been considered diagnostic for a protein-dominated sample (Brandes et al., 2004). Therefore, we observed not only amino acids, but extended peptides or protein chains that remain bonded after 66 m.y.

DISCUSSION

High-resolution PIC mapping and spectroscopy using PEEM analysis reveals significant similarities in shell microstructure and mineral composition between modern and ancient pinnid bivalve shells. A detailed comparison of the carbon K-edge XANES spectra from modern and Late Cretaceous IM shows some evidence of diagenetic alteration in the fossil shell (Fig. 2C): (1) The region of the spectrum between 289 and 300 eV associated with various amino acid side chains (Kaznacheyev et al., 2002) is enriched in the modern shell relative to the fossil; (2) the C=O and C-H peaks are both depleted in the Late Cretaceous shell with respect to the modern; and (3) the C=C peak is enhanced in the Late Cretaceous shell, due to the conversion of aliphatic (C-H) and carboxylic (C=O) carbon to aromatic (C=C) groups, as expected during diagenesis, and observed in plants and other fossils (e.g., Hare and Hoering, 1977; Boyce et al., 2003).

Despite this, the nearly identical energy position of the C=O peak at 288.1 eV in both shells demonstrates that we observe intact peptides preserved *in situ* over 66 m.y. Separate amino acids exhibit this peak at ~288.6 eV (Kaznacheyev et al., 2002; Myneni, 2002; Benzerara et al., 2006), whereas protein chains shift this peak to between 288.0 and 288.3 eV (Boese et al., 1997; Gordon et al., 2003; Brandes et al., 2004), due to de-shielding of the C=O group in a peptide bond, which lowers the peak energy (Boese et al., 1997; Gordon et al., 2003). Further, the observation of the C=O peak below 288.3 eV is quite unusual. There is evidence that glycine-rich peptides could induce a C=O peak *nearing* this energy position. Detailed spectroscopy of glycine peptides showed that there is a shift of the C=O peak position, from 288.6 eV for glycine (Kaznacheyev et al., 2002) to 288.3 eV in glycine trimers (Boese et al., 1997; Gordon et al., 2003). Thus, more than three adjacent glycine residues may plausibly shift the C=O peak to the energy position observed here. *Pinna* IM envelopes contain more than 40% glycine, thus the preservation of more than three adjacent glycine residues is feasible (Nakahara et al., 1980).

Chitin also shows a spectroscopic peak in this range, as observed by Cody et al. (2011) at 288.2 eV in Paleozoic arthropods, and Brandes et al. (2004) at 288.5 eV in marine particulate organic material. However, chitin spectra include a strong primary peak at 289.5 eV and a reduced-to-absent peak at 285.0 eV that does not match our spectra; instead, we observed a strong peak at 285.1 eV and a small-to-absent peak at 289.5 eV (Fig. 2C). Further, in a recent study of modern *Atrina* (sister genus of *Pinna*), chitin was observed within calcite prisms, but not the surrounding IM (Nudelman et al., 2007). Thus, although chitin is a more refractory organic compound, it cannot explain the unusual results described here.

The question then, is whether the glycine-rich IM formed as the animal deposited its shell, or as a result of taphonomic overprinting during diagenesis. Diagenetic glycinization occurs when the side chain of the original peptide is replaced by hydrogen during burial (Schweitzer, 2004). If this process increased the glycine concentration in the modern and fossil shells, it could not have occurred over geologic time scales. Instead, it may have occurred soon after the formation of the shell, prior to any influence from burial or fossilization (i.e., diagenesis), since the modern shell also shows the 288.1 eV peak and was collected alive in A.D. 1991 and analyzed 24 yr later. Notably, if glycinization occurs this rapidly, then nearly all shell proteins analyses, including modern samples, are likely to be equivalently biased.

Similarity in preserved microstructure and IM in a fossil and extant specimen from the same genus supports a primary, rather than modified, signal in these analyses. Consequently, the most likely explanation for the low energy position of the C=O peak is that the animal deposited glycine-rich proteins in the IM during life, and these have remained intact in nacre-grade shells over 66 m.y. This is supported by observations of high glycine concentrations in amino acid analyses of IM in extant *Pinna* shells and its sister genus *Atrina* (Bricteux-Grégoire et al., 1968; Nakahara et al., 1980; Dauphin et al., 2010), as well as other mollusks across 380 m.y. of Phanerozoic history (e.g., Wyckoff, 1972; Nakahara et al., 1980; Dauphin et al., 2010). Amino acid sequences from isolated IM proteins (e.g., Prismalin-14) demonstrate glycine concentrations of >15%–30% (Suzuki et al., 2004). It seems likely that space-filling carbonate minerals (Yang et al. 2011), including nacre tablets and calcite prisms, surround and protect organics from decay over time (Der Sarkissian et al., 2017). Such a process has been hypothesized for bone collagen and arthropod exoskeletons, even though both are more porous than carbonate shells (Cody et al., 2011; Lee et al., 2017). Nevertheless, whether of early taphonomic or primary origin, the presence of glycine-enriched IM in a 66 Ma bivalve indicates an exceptional quality of organic preservation in a nacre-grade fossil.

CONCLUSIONS

We present the first XANES spectroscopy analysis of mollusk shell microstructure and IM proteins using PEEM. Our findings indicate that the Late Cretaceous fossil retains original shell nacre, and prismatic layer mineralogy and microstructure, in conjunction with the preservation of peptides in the IM. Unusually low binding energy for the peptide carboxyl group C=O bond was observed, which can be explained by glycine-rich protein chains; amino acid analyses of modern and fossil bivalves demonstrate that glycine is prevalent in shell proteins (Nakahara et al., 1980; Suzuki et al., 2004; Dauphin et al., 2010).

This study, significantly, (1) provides the first direct observation of *in situ* protein chain preservation in marine invertebrates dating back to the Mesozoic; (2) documents glycine-rich protein chains, an important component of the IM in modern mollusks; (3) shows similar microstructure and IM preservation over 66 m.y. of evolutionary history within a single genus, and (4) demonstrates an exceptional quality of fossil organic preservation between the calcite prisms of nacre-grade shells, which are commonly preserved and easily identifiable. Because PEEM is performed *in situ*, it promises new horizons in studies of fossil skeletons. Moreover, given the fragility of DNA on geologic time scales, analyses of fossil proteins may prove important for reconstructing phylogenetic relationships and interpreting evolutionary history, paving the way for paleo-proteomics.

ACKNOWLEDGMENTS

We thank N. Landman, B. Hussaini, and G. Giribet for providing specimens, and S. Lemer, G. Falini, and Y. Dauphin for discussions. Support was provided by the NASA Astrobiology Institute and the NASA Postdoctoral Program (Myers, Knoll); the Harvard Society of Fellows (Bergmann); and by U.S. Department of Energy (Office of Science, Basic Energy Sciences, Chemical Sciences, Geosciences, and Biosciences Division) under Award DE-FG02–07ER15899, National Science Foundation grant DMR-1603192, and the Radcliffe Institute for Advanced Study (Gilbert). PEEM experiments were performed at the Advanced Light Source (Lawrence Berkeley National Laboratory), supported by grant DE-AC02–05CH11231.

REFERENCES CITED

Benzerara, K., Menguy, N., López-García, P., Yoon, T.-H., Kazmierczak, J., Tyliszczak, T., Guyot, F.,

and Brown, G.E., 2006, Nanoscale detection of organic signatures in carbonate microbialites: Proceedings of the National Academy of Sciences of the United States of America, v. 103, p. 9440–9445, https://doi.org/10.1073/pnas.0603255103.

Boese, J., Osanna, A., Jacobsen, C., and Kirz, J., 1997, Carbon edge XANES spectroscopy of amino acids and peptides: Journal of Electron Spectroscopy and Related Phenomena, v. 85, p. 9–15, https://doi.org/10.1016/S0368-2048(97)00032-7.

Boyce, K.C., Cody, G.D., Fogel, M.L., Hazen, R.M., Alexander, C., and Knoll, A.H., 2003, Chemical evidence for cell wall lignification and the evolution of tracheids in early Devonian plants: International Journal of Plant Sciences, v. 164, p. 691–702, https://doi.org/10.1086/377113.

Brandes, J.A., Lee, C., Wakeham, S., Peterson, M., Jacobsen, C., Wirick, S., and Cody, G., 2004, Examining marine particulate organic matter at sub-micron scales using scanning transmission X-ray microscopy and carbon X-ray absorption near edge structure spectroscopy: Marine Chemistry, v. 92, p. 107–121, https://doi.org/10.1016/j.marchem.2004.06.020.

Bricteux-Grégoire, S., Florkin, M., and Grégoire, C., 1968, Prism conchiolin of modern or fossil molluscan shells: An empire of protein paleization: Comparative Biochemistry and Physiology, v. 24, p. 567–572, https://doi.org/10.1016/0010-406X(68)91009-8.

Cody, G.D., Gupta, N.S., Briggs, D.E., Kilcoyne, A., Summons, R.E., Kenig, F., Plotnick, R.E., and Scott, A.C., 2011, Molecular signature of chitin-protein complex in Paleozoic arthropods: Geology, v. 39, p. 255–258, https://doi.org/10.1130/G31648.1.

Dauphin, Y., Brunelle, A., Cotte, M., Cuif, J., Farre, B., Laprévote, O., Meibom, A., Salomé, M., and Williams, C., 2010, A layered structure in the organic envelopes of the prismatic layer of the shell of the pearl oyster *Pinctada margaritifera* (Mollusca, Bivalvia): Microscopy and Microanalysis, v. 16, p. 91–98, https://doi.org/10.1017/S1431927609991115.

De Jong, E., Westbroek, P., Westbroek, J., and Bruning, J., 1974, Preservation of antigenic properties of macromolecules over 70 Myr: Nature, v. 252, p. 63–64, https://doi.org/10.1038/252063a0.

Der Sarkissian, C., Pichereau, V., Dupont, C., Ilsøe, P.C., Perrigault, M., Butler, P., Chauvaud, L., Eiriksson, J., Scourse, J., and Paillard, C., 2017, Ancient DNA analysis identifies marine mollusc shells as new metagenomic archives of the past: Molecular Ecology Resources, v. 17, p. 835–853, https://doi.org/10.1111/1755-0998.12679.

Gilbert, P.U., Bergmann, K.D., Myers, C.E., Marcus, M.A., DeVol, R.T., Sun, C.-Y., Blonsky, A.Z., Tamre, E., Zhao, J., and Karan, E.A., 2017, Nacre tablet thickness records formation temperature in modern and fossil shells: Earth and Planetary Science Letters, v. 460, p. 281–292, https://doi.org/10.1016/j.epsl.2016.11.012.

Gilbert, P.U.P.A., Metzler, R.A., Zhou, D., Scholl, A., Doran, A., Young, A., Kunz, M., Tamura, N., and Coppersmith, S.N., 2008, Gradual ordering in red abalone nacre: Journal of the American Chemical Society, v. 130, p. 17519–17527, https://doi.org/10.1021/ja8065495.

Gilbert, P.U.P.A., Young, A., and Coppersmith, S.N., 2011, Measurement of c-axis angular orientation in calcite ($CaCO_3$) nanocrystals using x-ray absorption spectroscopy: Proceedings of the National Academy of Sciences of the United States of America, v. 108, p. 11350–11355, https://doi.org/10.1073/pnas.1107917108.

Gordon, M.L., Cooper, G., Morin, C., Araki, T., Turci, C.C., Kaznatcheev, K., and Hitchcock, A.P., 2003, Inner-shell excitation spectroscopy of the peptide bond: Comparison of the C 1s, N 1s, and O 1s spectra of glycine, glycyl-glycine, and glycyl-glycyl-glycine: The Journal of Physical Chemistry A, v. 107, p. 6144–6159, https://doi.org/10.1021/jp0344390.

Grégoire, C., and Voss-Foucart, M.-F., 1970, Proteins in shells of fossil cephalopods (Nautiloids and Ammonoids) and experimental simulation of their alterations: Archives Internationales de Physiologie et de Biochimie, v. 78, p. 191–203, https://doi.org/10.3109/13813457009103797.

Hare, P., and Hoering, T., 1977, The organic constituents of fossil mollusc shells: Carnegie Institute of Washington Year Book, v. 78, p. 625–631.

Jope, M., 1969, The protein of brachiopod shell—IV. Shell protein from fossil inarticulates: Amino acid composition and disc electrophoresis of fossil articulate shell protein: Comparative Biochemistry and Physiology, v. 30, p. 225–232, https://doi.org/10.1016/0010-406X(69)90806-8.

Kaznacheyev, K., Osanna, A., Jacobsen, C., Plashkevych, O., Vahtras, O., Ågren, H., Carravetta, V., and Hitchcock, A., 2002, Innershell absorption spectroscopy of amino acids: The Journal of Physical Chemistry A, v. 106, p. 3153–3168, https://doi.org/10.1021/jp013385w.

Lee, Y.-C., Chiang, C.-C., Huang, P.-Y., Chung, C.-Y., Huang, T.D., Wang, C.-C., Chen, C.-I., Chang, R.-S., Liao, C.-H., and Reisz, R.R., 2017, Evidence of preserved collagen in an Early Jurassic sauropodomorph dinosaur revealed by synchrotron FTIR microspectroscopy: Nature Communications, v. 8, p. 14220, https://doi.org/10.1038/ncomms14220.

Metzler, R.A., Tribello, G.A., Parrinello, M., and Gilbert, P., 2010, Asprich peptides are occluded in calcite and permanently disorder biomineral crystals: Journal of the American Chemical Society, v. 132, p. 11585–11591, https://doi.org/10.1021/ja103089r.

Muyzer, G., and Westbroek, P., 1989, An immunohistochemical technique for the localization of preserved biopolymeric remains in fossils: Geochimica et Cosmochimica Acta, v. 53, p. 1699–1702, https://doi.org/10.1016/0016-7037(89)90255-X.

Myneni, S.C., 2002, Soft X-ray spectroscopy and spectromicroscopy studies of organic molecules in the environment: Reviews in Mineralogy and Geochemistry, v. 49, p. 485–579, https://doi.org/10.2138/gsrmg.49.1.485.

Nakahara, H., Kakei, M., and Bevelander, G., 1980, Fine structure and amino acid composition of the organic envelope in the prismatic layer of some bivalve shells: Venus (Fukuyama-Shi, Japan), v. 39, p. 167–177.

Nudelman, F., Chen, H.H., Goldberg, H.A., Weiner, S., and Addadi, L., 2007, Spiers Memorial Lecture lessons from biomineralization: Comparing the growth strategies of mollusc shell prismatic and nacreous layers in *Atrina rigida*: Faraday Discussions, v. 136, p. 9–25, https://doi.org/10.1039/b704418f.

Olson, I.C., Blonsky, A.Z., Tamura, N., Kunz, M., and Gilbert, P.U.P.A., 2013, Crystal nucleation and near-epitaxial growth in nacre: Journal of Structural Biology, v. 184, p. 454–463, https://doi.org/10.1016/j.jsb.2013.10.002.

Orlando, L., Ginolhac, A., Zhang, G., Froese, D., Albrechtsen, A., Stiller, M., Schubert, M., Cappellini, E., Petersen, B., and Moltke, I., 2013, Recalibrating *Equus* evolution using the genome sequence of an early Middle Pleistocene horse: Nature, v. 499, p. 74, https://doi.org/10.1038/nature12323.

Schroeter, E.R., DeHart, C.J., Cleland, T.P., Zheng, W., Thomas, P.M., Kelleher, N.L., Bern, M., and Schweitzer, M.H., 2017, Expansion for the *Brachylophosaurus canadensis* collagen I sequence and additional evidence of the preservation of Cretaceous protein: Journal of Proteome Research, v. 16, p. 920–932, https://doi.org/10.1021/acs.jproteome.6b00873.

Schweitzer, M.H., 2004, Molecular paleontology: some current advances and problems: Annales de Paléontologie, v. 90, p. 81–102, https://doi.org/10.1016/j.annpal.2004.02.001.

Stöhr, J., 2013, NEXAFS Spectroscopy: Springer Series in Surface Sciences, v. 25: Berlin Heidelberg, Springer-Verlag, 404 p., https://doi.org/10.1007/978-3-662-02853-7.

Suzuki, M., Murayama, E., Inoue, H., Ozaki, N., Tohse, H., Kogure, T., and Nagasawa, H., 2004, Characterization of Prismalin-14, a novel matrix protein from the prismatic layer of the Japanese pearl oyster (*Pinctada fucata*): The Biochemical Journal, v. 382, p. 205–213, https://doi.org/10.1042/BJ20040319.

Vendrasco, M.J., Checa, A., Heimbrock, W.P., and Baumann, S.D., 2013, Nacre in molluscs from the Ordovician of the Midwestern United States: Geosciences, v. 3, p. 1–29, https://doi.org/10.3390/geosciences3010001.

Weiner, S., Lowenstam, H., and Hood, L., 1976, Characterization of 80-million-year-old mollusk shell proteins: Proceedings of the National Academy of Sciences of the United States of America, v. 73, p. 2541–2545, https://doi.org/10.1073/pnas.73.8.2541.

Wyckoff, R.W.G., 1972, Biochemistry of Animal Fossils: Bristol, UK, Scientechnica, 152 p.

Yang, L., Killian, C.E., Kunz, M., Tamura, N., and Gilbert, P., 2011, Biomineral nanoparticles are space-filling: Nanoscale, v. 3, p. 603–609, https://doi.org/10.1039/C0NR00697A.

Zhao, H., Samata, T., Takakura, D., Hashimoto, R., Miyazaki, Y., Nosawa, T., and Hikita, Y., 2003, Organic matrix proteins preserved in fossil molluscan shells, *in* Kobayashi, I., and Ozawa, H., eds., Biomineralization: Formation, Diversity, Evolution and Application: Kanagawa, Japan, Tokai University Press, p. 108–111.

Manuscript received 20 November 2017
Revised manuscript received 28 June 2018
Manuscript accepted 28 June 2018

Printed in USA